Image enhancement for a low cost TEM acquisition system.

Gregory Randall[a], Alicia Fernández[a], Omar Trujillo-Cenóz[b], Gustavo Apelbaum[a], Marcelo Bertalmío[a], Luis Vázquez[a], Francisco Malmierca[a] and Pablo Morelli[a]

[a]Instituto de Ingeniería Eléctrica, Facultad de Ingeniería, Universidad de la República
Julio Herrera y Reissig 565, Montevideo, Uruguay

[b]Instituto de Investigaciones Biológicas Clemente Estable
Ave. Italia 3318, Montevideo, Uruguay

ABSTRACT

This paper describes a method for the improvement of biological images acquired using a Transmission Electronic Microscope (TEM). Several techniques are presented that deal with noise reduction, artifact removal and non-uniform illumination correction. Experimental results are shown.

Keywords: Transmission Electronic Microscopy, image processing, non-uniform illumination.

1. INTRODUCTION

Since 1995 there has been intense cooperation between two research teams: the Compared Neuroanatomy Division at the Instituto de Investigaciones Biológicas Clemente Estable and the Image Processing Group at the Instituto de Ingeniería Eléctrica of the Facultad de Ingeniería, Montevideo, Uruguay. The main goal of this joint effort is the creation of a platform that may assist the neurobiologists in the creation of three dimensional models of nervous tissue observed through a TEM. A general description of the project can be found in,[1] but here we shall condense the experimental procedure in order to outline the subject of this paper:

1. A neuron's activity is registered in a certain region of the Central Nervous System. This neuron may be marked by a colorant substance injected in the tissue.
2. A portion of nervous tissue is extracted from the animal. This tissue is dehydrated and embedded in plastic epoxy for its hardening.
3. The hardened tissue is sliced into very thin sections (800 to 1000 Å).
4. The slices are observed through a TEM. A CCD camera mounted on the outside of the binocular glass is used to take images that are digitized and stored in the hard disk of the acquiring station.
5. A skilled biologist marks the boundaries of the region of interest in each slice, using the Graphic User Interface (GUI).
6. The program achieves automatic registration of the slices, finding their relative locations and orientations.
7. The slices are piled up properly, and a 3D model is displayed.

In this paper we will discuss the algorithms developed for the improvement of the images (item 4), prior to segmentation, registration and 3D rendering. In a system such as this one, the quality of the final result is strongly dependent on the quality of the signal at its early stages.

Other author information: (Send correspondence to G.R.)
G.R.: Email: randall@iie.edu.uy; Telephone: (+5982) 711-0974; Fax: (+5982) 711-7435;
A. F.: Email: alicia@iie.edu.uy; Telephone: (+5982) 711-0974; Fax: (+5982) 711-7435;
Supported by the CSIC, UR.

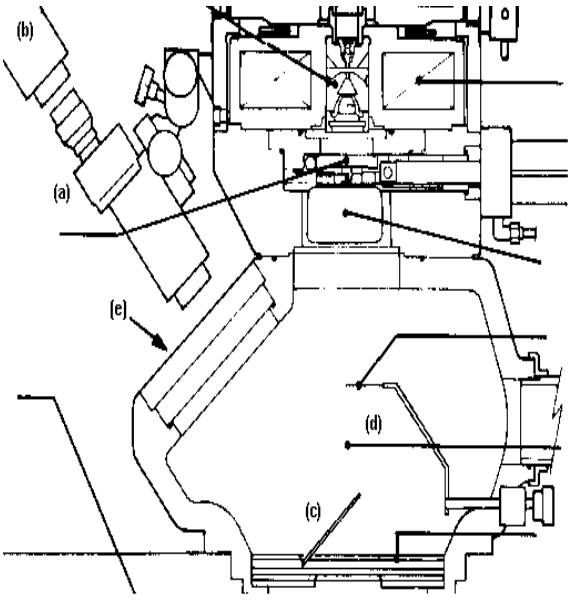

Figure 1. Section scheme of part of a Transmission Electronic Microscope. **(a)** Focus adjustment binocular glass. **(b)** CCD camera for direct image acquisition. **(c)** Phosphorescent plate on which the image is projected. **(d)** Zone of passage for the electron beam. **(e)** Thick glass. **(f)** Photographic camera.

2. THE PROBLEM

The first step for this computer-aided three dimensional neuron reconstruction system is the acquisition of the images. Several alternatives were considered,[1] and finally a direct acquisition platform was chosen. This platform consists of:

- A CCD camera mounted on the binocular used by the biologist for focus adjustment.
- A PC with a digitizer board.
- A software to control the acquisition board allowing the user to capture a sequence of images, through its GUI.

The position of the CCD camera in the TEM is illustrated by figure 1. This low-cost platform reduces drastically the amount of time required to acquire a sequence. Its drawback comes from the fact that the images are acquired through an optical system designed not to take high quality images but to allow focus adjustment:

- The electronic beam activates the luminescent phosphor of a plate on which the image is projected, releasing photons.
- These photons go through a very thick glass, designed to shield the user from fallout and to resist high vacuum.
- The image is viewed through the binocular glass, allowing the user to adjust the focus.
- The CCD camera is mounted on the binocular glass.

Under these conditions several perturbations appear:

1. Thermo electrical noise, related to the image acquisition in low luminance conditions.

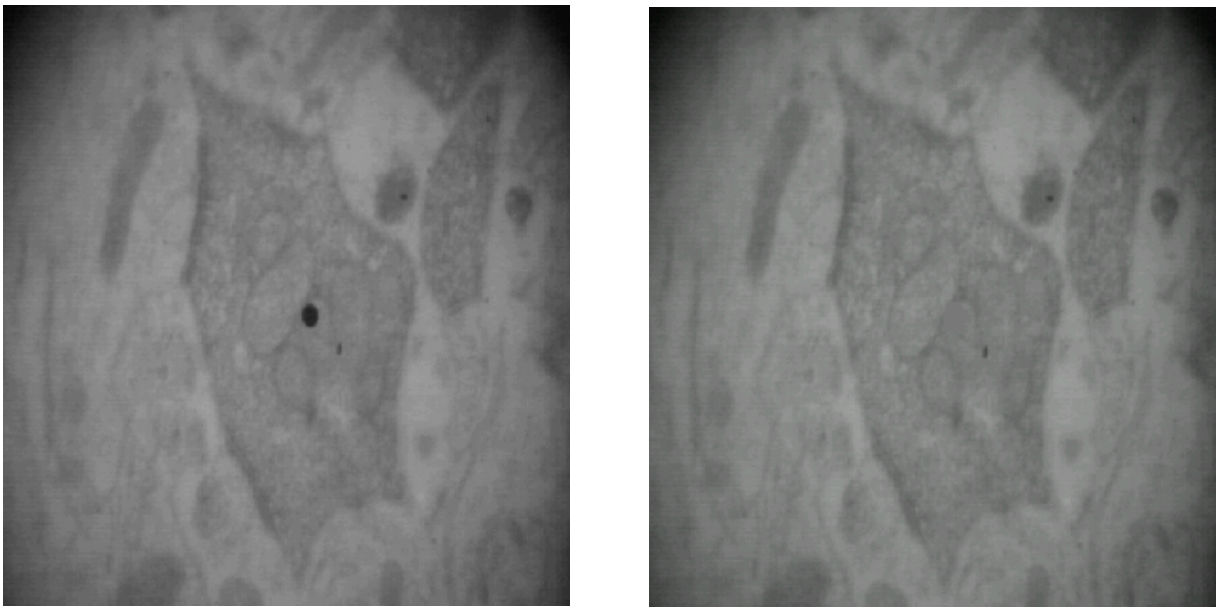

Figure 2. Right: Image obtained by means of direct acquisition, with 4-images averaging and illumination adjustment with real-time histogram. Left: Same image, after the focus adjustment circle removal.

2. The phosphor plate has a black circle for the focus adjustment. This circle is present on the images, and its size is not negligible (see figure 2).
3. The electronic beam is concentrated on **c** to activate the phosphor, thus granting that an image is formed on the CCD sensor. This concentration of the beam causes the illumination to be non uniform over the image.
4. Geometrical deformation caused by the glasses through which the image is taken.
5. The image is also affected by the non uniform sensitivity of the CCD cells.

The problem is then to devise ways of compensating these distortions. In this paper we will address the first three points.

3. THERMO ELECTRICAL NOISE

We assume that the thermo electrical noise present when acquiring an image is a random signal with Gaussian distribution, variance s and zero mean, added to the tissue signal or "clean" signal. We also assume that the "clean" signal is time invariant (thus neglecting the thermal drift).

It is then straightforward to see that an average of N images will keep the mean of the noise of the resulting image but its variance s will be reduced to $s/\sqrt{N}$.[2] Figure 2 depicts the result of real-time averaging.

In order to increase the number of grey levels present in the image, a real-time histogram of the region of interest is displayed. It allows the user to adjust the illumination level to avoid saturation while increasing the gray gamut.

4. FOCUS ADJUSTMENT CIRCLE

This black circle is present due to the fact that this images are taken directly from the binocular glass. The circle does not appear on photographs since the plate where it is located on, is removed letting pass the electronic beam to impact the photographic film.

This circle hides un-retrievable information. It also occupies several grey levels, hence its elimination allows contrast enhancement of the image.

An algorithm was devised for this purpose. First, the circle is located by a correlation scheme with the use of a synthetic image that approximates the shape of the circle. Then the points within the circle are replaced by an average of the neighboring region.

This black circle removal may be helpful for the registration stage that will take place later on, since the black circle has no relation with the biological information and it may mislead the registration algorithm. Figure 2 shows one slice before and after circle removal.

5. NON-UNIFORM ILLUMINATION

The cause of this problem can be seen observing figure 1. The TEM was designed for the photographic acquisition of images, and thus after the biologist has adjusted the focus by looking at the image formed on the plate **c**, the plate is withdrawn so that the electronic beam impacts the photographic film. Since the choice was made (for the system to be low-cost) of placing the CCD camera on one of the binocular glasses, the plate is no longer removed when taking an image. The electronic beam must be concentrated so as to reach the plate with the intensity required for the image formed on the plate to be captured by the CCD camera. Hence the illumination is no longer homogeneous over the image, unlike when the image was taken on photographic film.

We assume[2] that the image $\mathcal{A}$ is the product of a $\mathcal{B}$ signal (the reflectance component, or 'useful' signal) by another signal, $\mathcal{I}$ (the illumination signal):

$\mathcal{A} = \mathcal{B}\mathcal{I}$

Since the illumination is non-uniform, $\mathcal{I}$ is not constant but a function of the coordinates.

In order to obtain $\mathcal{B}$, having $\mathcal{A}$, we must estimate $\mathcal{I}$. This estimation will take into account two characteristics of $\mathcal{I}$ that come from the observation of the images:

1. Its shape is not random, but determined by the shape of the beam. It is a continuous function that must be approximated.
2. The perturbation $\mathcal{I}$ is more important than $\mathcal{B}$. This fact can be seen on figures 2 and 3. Now we will describe several methods for the estimation of $\mathcal{I}$.

6. APPROXIMATION OF $\mathcal{I}$ WITH A QUADRATIC FORM

The image $\mathcal{A}$ is divided in nxn rectangles. We assume that $1/n$ is:

- Small enough to assume $\mathcal{I}$ approximately constant over each rectangle.
- Big enough to assume $\mathcal{B}$ has on each rectangle the same mean value.

We also assume that $\mathcal{B}$ and $\mathcal{I}$ are independent. Hence we can use the mean value on each rectangle as a measure proportional to $\mathcal{I}$. The estimation is more robust if we assume a certain shape for $\mathcal{I}$, thus reducing the influence of noise and the signal $\mathcal{B}$ in our approximation of $\mathcal{I}$. We chose a quadratic form for $\mathcal{I}$:

$\mathcal{I}(x,y) = a_0 + a_1 x + a_2 y + a_3 xy + a_4 x^2 + a_5 y^2$

The method consists of the estimation of the a_i coefficients of this polynomial. With nxn samples, we get nxn equations and we can solve for a_i by the minimum squares method.

Figure 4 shows the results obtained. It is evident that the estimation error is greater at the center of the picture, due to the deviation of $\mathcal{I}$ from a quadratic form in this region. Nevertheless, this methods provides a very good means of estimation of the center of $\mathcal{I}$. This will be used in the next two methods.

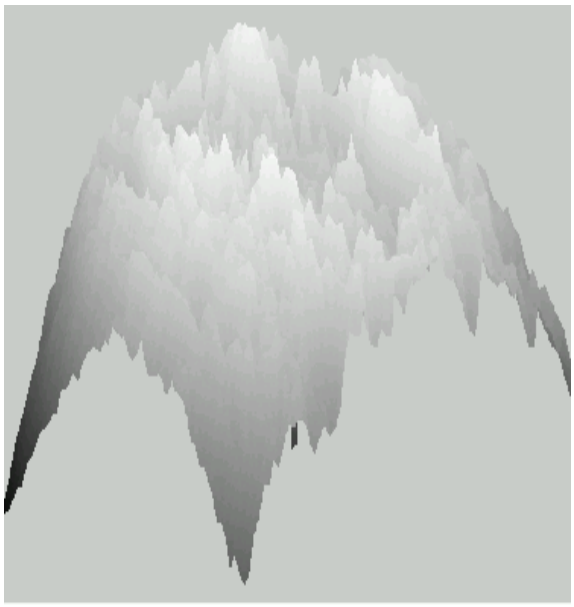

Figure 3. 3D graph plot of the figure 2 image. Grey levels correspond to Z coordinates. Notice the importance of non-uniform illumination.

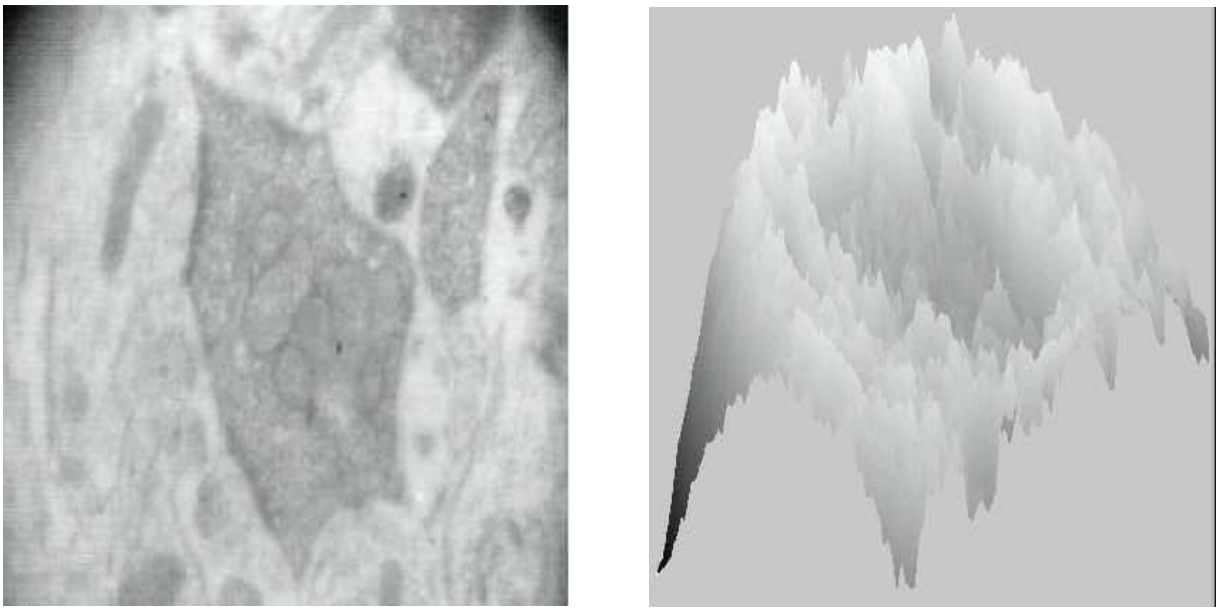

Figure 4. The result of correcting image from figure 2 with the quadratic form method. Left:3D graph plot of the image. Grey levels correspond to Z coordinates. Notice the sinking on the middle of the image, due to the quadratic form assumption.

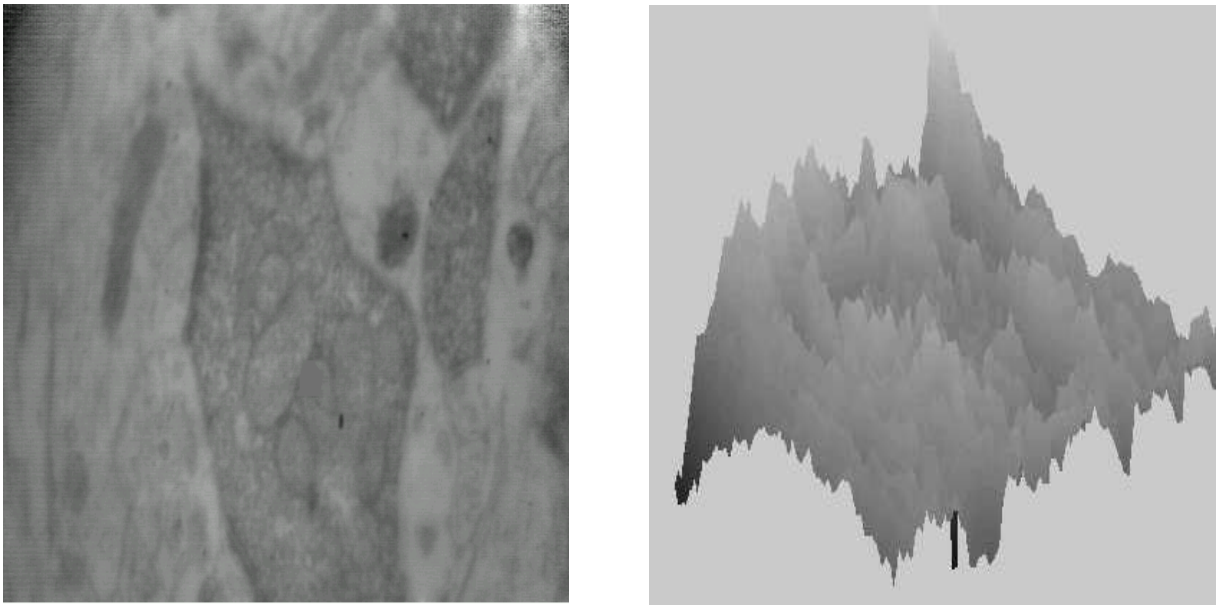

Figure 5. Image from figure 2 corrected by means of the radial method. Left: 3D graph plot of the corrected image. Grey levels correspond to Z coordinates.

7. RADIAL METHOD

A more accurate description of $\mathcal{I}$ would be that of a revolution surface slightly flattened at its center, rather than a quadratic form. This method deals then with the estimation of the generatrix $\mathcal{I}(r)$ of this surface. An immediate advantage is the reduction of the problem to a one-dimensional one.

We must first estimate the location of the center $\mathcal{O}$ of the surface ($r = 0$); this can be accomplished quite accurately with the quadratic form method described in the previous paragraph. Then we define concentric rings, centered at $\mathcal{O}$, with variable radius. The value of $\mathcal{I}$ over each ring is estimated as the mean value of $\mathcal{A}$ over that ring, as we did in the previous method with the rectangles. The estimation of $\mathcal{I}$ thus accomplished improves that of the quadratic form method for at least two reasons:

1. Averaging over rings diminishes the influence of $\mathcal{B}$ on our measure.
2. The shape of $\mathcal{I}$ is not assumed, apart from its radial characteristic.

Once we have an estimation of $\mathcal{I}(r)$ for each ring, the continuous function $\mathcal{I}(r)$ is interpolated with cubic splines, granting continuity to the second derivative. Figure 5 shows the results obtained for the image in figure 2.

8. HISTOGRAM METHOD

The best estimation possible of the $\mathcal{I}$ signal for a given image $\mathcal{A}$ is that obtained when, during the acquisition process, the tissue from which $\mathcal{A}$ is taken is removed from the plate and the resulting image is taken (without changing focus, magnification, beam intensity or any other parameter): this is an image very close to the 'pure illumination' image $\mathcal{I}$ we are looking for. The similarity between the histograms of both $\mathcal{A}$ and this related image is remarkable. In fact, if the second hypothesis we formulated concerning $\mathcal{I}$ is true, then the histogram of $\mathcal{A}$ will be strongly dependent to $\mathcal{I}$.

The histogram method estimates $\mathcal{I}$ from $\mathcal{A}$ assuming that:

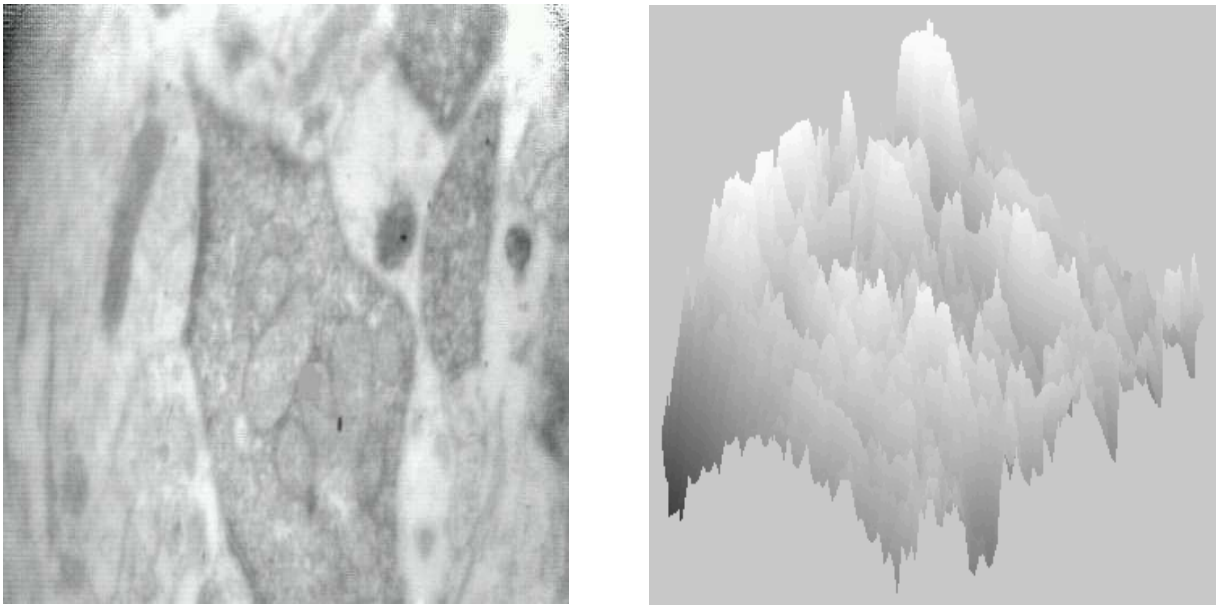

Figure 6. Image from figure 2 corrected by means of the histogram method. Right: 3D graph plot.Grey levels correspond to Z coordinates.

- the histogram of $\mathcal{A}$ is a good estimate of the histogram of $\mathcal{I}$.
- $\mathcal{I}$ is a revolution surface.
- $\mathcal{I}(r)$ is monotony decreasing, hence every $\mathcal{I}_i$ has a corresponding radius r_i.

Given these hypothesis we can state that:

$N(\mathcal{I}_i) = \pi r^2(\mathcal{I}_i)$

where

- $\mathcal{I}_i$ is a value of intensity of $\mathcal{I}$,
- $r(\mathcal{I}_i)$ is the radius corresponding to $\mathcal{I}_i$,
- $N(\mathcal{I}_i)$ is the number of points of the image with intensity between $\mathcal{I}_i$ and $\mathcal{I}_{max}$.
- $\mathcal{I}_{max}$ is the intensity corresponding to the center $\mathcal{O}$ of $\mathcal{I}$.

The first member of this equation is the integral of the histogram over the interval $(\mathcal{I}_i, \mathcal{I}_{max})$. Hence, integration of the histogram of $\mathcal{A}$ gives us all the values of $N(\mathcal{I}_i)$, from which $r(\mathcal{I}_i)$ and consequently $\mathcal{I}_i$ can be easily computed.

The simplicity of this method may make it suitable for real-time illumination compensation. Figure 6 shows the results of applying this method to the image on figure 2. Figure 7 shows that this method is highly sensitive to the estimation of the center $\mathcal{O}$. We use the quadratic form method for the location of this point.

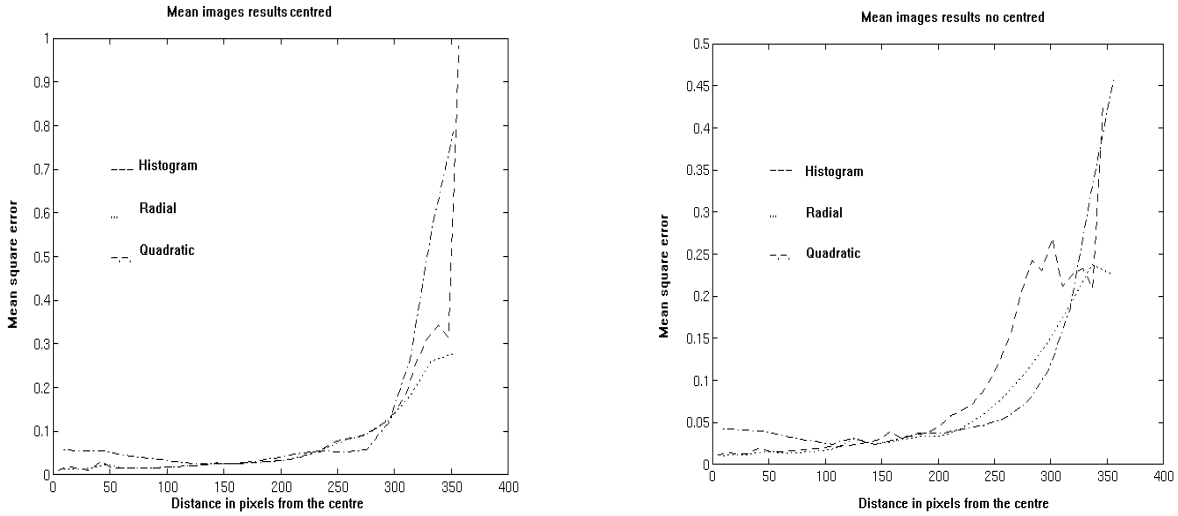

Figure 7. Right: Mean square error of non-uniform illumination correction vs. distance from the center of the illumination signal. Averaged results of 3 centered 'pure illumination' images.Left: Mean square error of non-uniform illumination correction vs. distance from the center of the illumination signal. Averaged results of 9 non centered 'pure illumination' images. Notice how the results are poorer for the histogram method for distances greater than 200 (corresponding to the limit where the concentric rings are contained in the image).

9. EXPERIMENTAL RESULTS

In order to compare the results obtained with each of the methods depicted above, we proceed as follows:

- We take as image $\mathcal{A}$ an image of 'pure illumination', that is, an image acquired without the presence of biological tissue.
- The mean square error between the quotient $\mathcal{A}/\mathcal{I}$ and a plane is computed.
- This error is plotted versus the distance (in pixels) from the point $\mathcal{O}$.

Since $\mathcal{A}$ is a 'pure illumination' image, the estimation $\mathcal{I}$ should be identical to $\mathcal{A}$, so a perfect correction implies that $\mathcal{A}/\mathcal{I}$ is a plane. We plot an average of the error computed over rings concentric with $\mathcal{O}$, so that we can see the dependency of these methods with the distance to the center of $\mathcal{I}$.

These measures were taken for several images and the averaged results are shown on figure 7. It can be noticed how the quadratic form method carries greater error on the middle region of the image, the region of interest.

The left graphic in figure 7 shows the results obtained for images where the point $\mathcal{O}$ is quite apart from the image center. In this case, the histogram method carries a more significant error.

Figures 3 to 6 shows a 3D graph representation of the images, where the grey level is plotted on the Z axis. These figures shows how the original image illumination component is 'flattened' while preserving the shape of the signal of interest. Results are poorer on the corners, where the information is lost due to black saturation. Figure 4 shows the sinking of the middle region due to the assumption of a quadratic form for $\mathcal{I}$.

REFERENCES

1. G. Randall, A. Fernandez, O. Trujillo-Cenoz, G. Apelbaum, M. Bertalmio, L. Vazquez, F. Malmierca, and P. Morelli, "Neuro3d:an interactive 3d reconstruction system of serial sections using automatic registration," SPIE, January 1998.
2. R. C. Gonzales and R. E. Woods, *Digital Image Processing*, Addison Wesley, 1993.